Electronic Supplementary Material (ESI) for Physical Chemistry Chemical Physics

Supplementary Information

Fabrication of graphene/carbon nanotube paper decorated with nanoneedle manganese oxide on the outermost graphene sheets for supercapacitors

By Myeongjin Kim, Yongseon Hwang and Jooheon Kim*

*Corresponding author: Prof. Jooheon Kim

School of Chemical Engineering & Materials Science,

Chung-Ang University, Seoul 156-756, Korea

E-mail: jooheonkim@cau.ac.kr

1. FE-SEM images of C-GCP

The microscopic appearance of C-GCP was examined by scanning electron microscopy (SEM). Fig. S1 shows cross-sections of C-GCP with different CNT contents uniformly intercalated between well-aligned GO layers. The structure of C-GCP form stacked paper-like structure, composed of abundant thin stacks of a few sheets of monolayer GO. It is clear that, with the increase of CNT content in the C-GCP, the intercalation of CNT is more common. The role of CNT were to physically separate the graphene layers and thus to create a well-defined porous sandwich structure. These graphene/CNT sandwich papers are considered more promising electrochemically than the neat graphene papers because the interlayer distance in the neat graphene paper is too narrow for ions to intercalate.

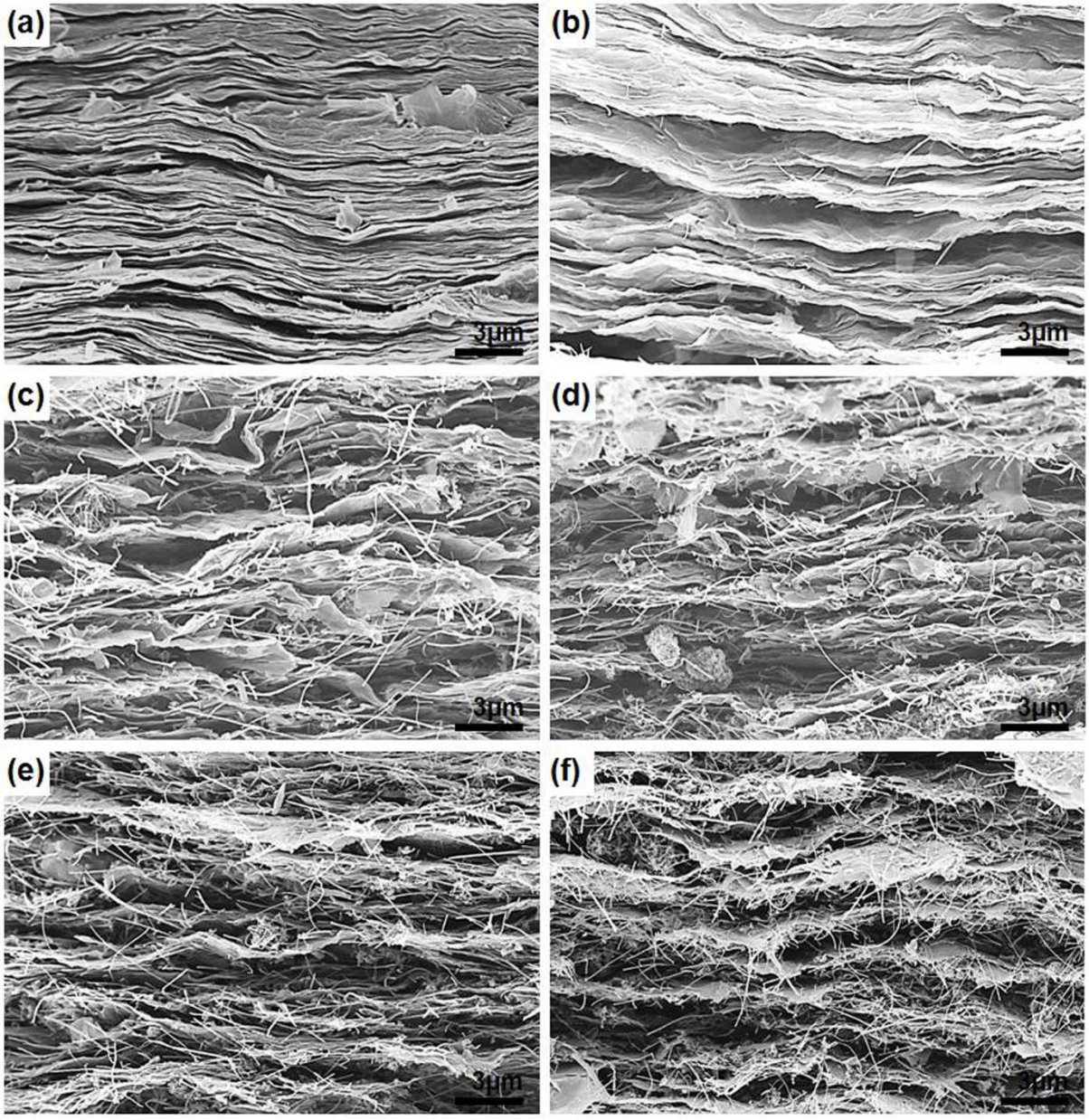

Fig. S1.FE-SEM images of (a) neat GO paper, and C-GCP with different CNT contents of (b) 5 wt.%, (c) 10 wt.%, (d) 15 wt.%, (e) 20 wt.% and (f) 30 wt.%.

2. Investigation of the degree of reduction for C-GCP/MnO_2

To investigate the degree of reduction, the composition of heterocarbon was analyzed based on the deconvoluted C 1s core-level spectra of C-GCP10/MnO_2(6) and C-rGCP10/MnO_2(6). Fig. S2(a) and (b) show the deconvoluted C 1s core-level spectra of C-GCP10/MnO_2(6) and C-rGCP10/MnO_2(6), respectively.

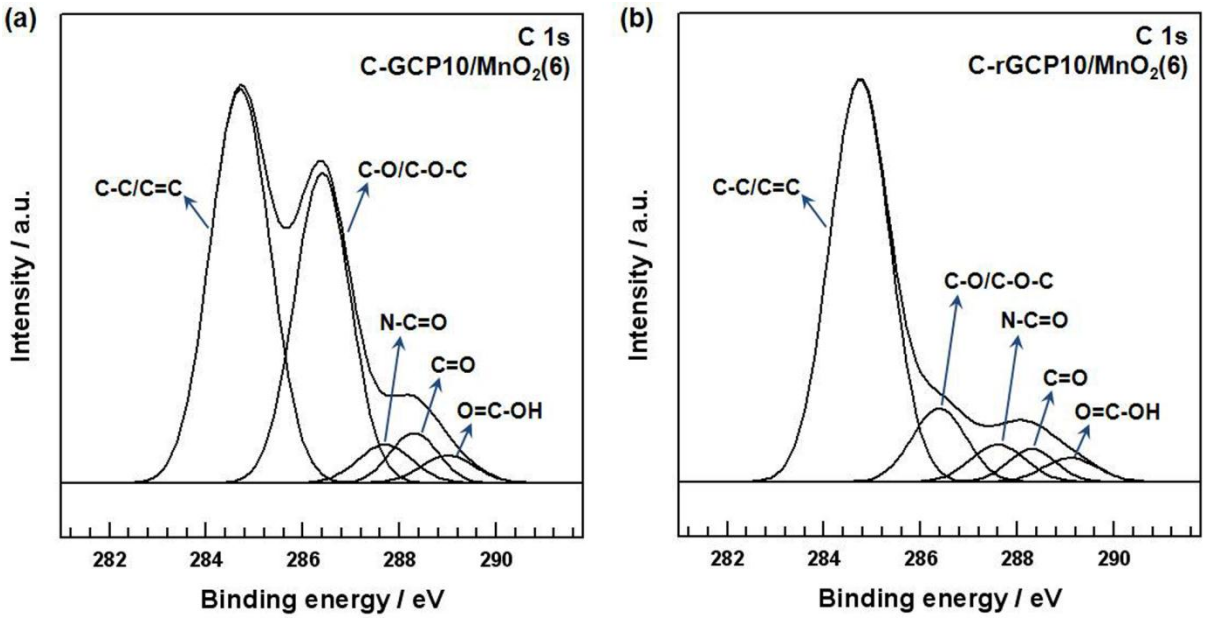

Fig. S2.XPS spectra of C-GCP10/MnO_2(6) and C-rGCP10/MnO_2(6).

(a) XPS C 1s spectra of C-GCP10/MnO_2(6) and (b) XPS C 1s spectra of C-rGCP10/MnO_2(6)

C-GCP10/MnO_2(6) exhibited strong aromatic C-C/C=C and –C-OH/C-O-C binding energy peaks at 284.7 and 286.4 eV, respectively, with several binding energy peaks corresponding with oxygen-containing functional groups such as C=O at 288.3 eV and O-C=O at 289.0 eV as well as amide functional groups such as N-C=O at 287.7 eV. Compared with C-GCP10/MnO_2(6), the area of the peak associated with C-C/C=C was predominant in the C 1s spectrum of C-rGCP10/MnO_2(6), while those of C-O, C=O, and O=C-OH were dramatically decreased. Therefore, the heterocarboncomponent of C-rGCP10/MnO_2(6) (24.2 %) was markedly decreased compared with that of C-GCP10/MnO_2(6) (49.9 %), indicating that thermal reduction effectively removed oxygen functional groups. Table S1 summarizes the differences of the C-GCP10/MnO_2(6) and C-rGCP10/MnO_2(6) in terms of their elemental composition.

	Fitting of the C 1s peak Binding energy eV (relative atomic percentage %)				
	C-C/C=C	C-O/C-O-C	N-C=O	C=O	O=C-OH
C-GCP10/MnO_2(6)	284.7 (50.1)	286.4 (37.1)	287.7 (4.5)	288.3 (5.1)	289 (3.2)
C-rGCP10/MnO_2(6)	284.7 (75.8)	286.3 (12.3)	287.6 (4.3)	288.3 (4.8)	289.1 (2.8)

Table S1

3. Dispersion features of C-GCP

Fig. S3 revealed the dispersion features of the C-GCP10 in the DMF and IPA, respectively in the same conditions (150 rpm, until 50 min). Fig. S3(a) showed the immersion of C-GCP10 in the IPA as time passes. In this case, C-GCP10 was not affected by IPA during the mild stirring due to small electrical dipole moments of IPA. Therefore, MnO_2 decorated on the outermost GO layers during the reaction without exfoliation. In the case of reaction in the DMF (Fig. S3(b)), C-GCP10 was broken after 2 min. due to large electrical dipole moment of the DMF, which provided short term stability in the C-GCP10.

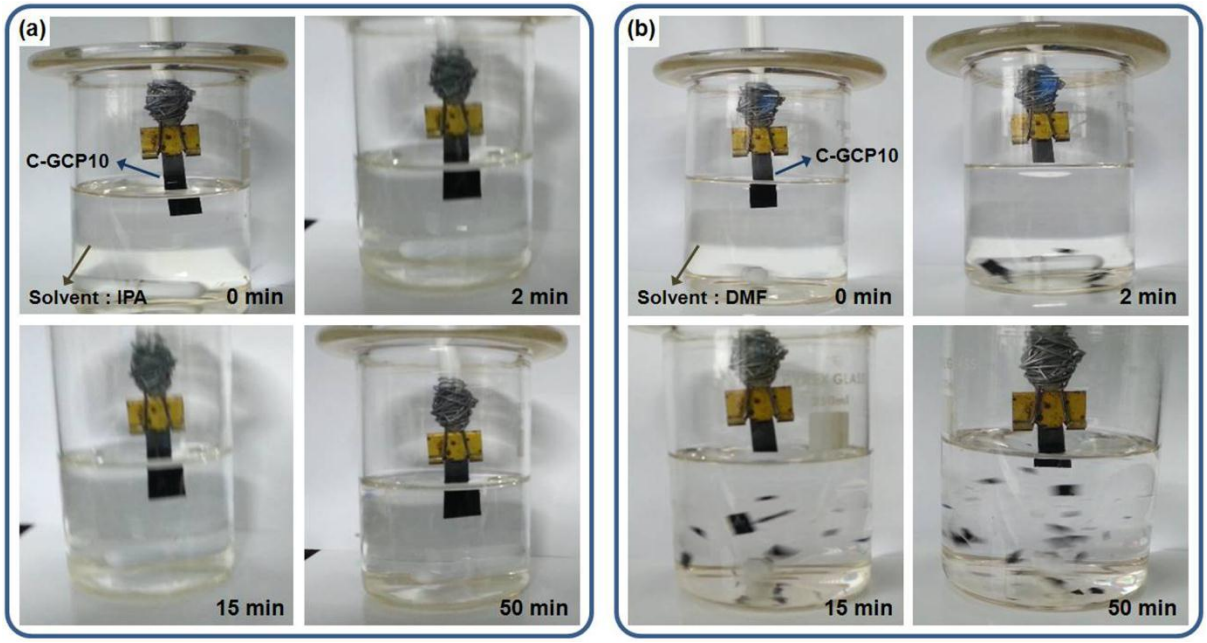

Fig. S3. Dispersion features of C-GCP10 in the DMF and IPA